PHYSICAL REVIEW B VOLUME 18, NUMBER 12 15 DECEMBER 1978

Thermally induced effects in evaporated chalcogenide films. I. Structure

R. J. Nemanich, G. A. N. Connell, T. M. Hayes, and R. A. Street
Xerox Palo Alto Research Center, 3333 Coyote Hill Road, Palo Alto, California 94304
(Received 17 July 1978)

The structure of evaporated As_2S_3, As_2Se_3, and $GeSe_2$ films, and the influence of annealing at the glass-transition temperature, are studied by extended x-ray-absorption fine structure (EXAFS) and by Raman spectroscopy. In addition, the topology of each film is analyzed by calculating the x-ray diffraction for several models. The films were prepared by evaporation onto substrates held near room temperature. All the as-deposited films exhibited significant homopolar bonding in contrast to the almost totally heteropolar bonding of the corresponding bulk quenched glasses. Upon annealing of the films, the measurements indicate that the density of homopolar bonds decreases, and the films more closely resemble the bulk quenched glasses. The Raman spectra are quantitatively analyzed with two models to characterize the disorder, and then compared to the EXAFS results. The analysis indicates an As-As coordination of ~ 0.6 and ~ 0.4 and a Ge-Ge coordination of ~ 0.3 for the As_2S_3, As_2Se_3, and $GeSe_2$ as-deposited films, respectively. The measurements also indicate that the As-As bonds of the As_2S_3 film are incorporated into S_2As-AsS_2 units, suggesting the presence of As_4S_4 molecules. Calculations using this model are in good agreement with x-ray diffraction data in the literature. The data from As_2Se_3 evaporated films also indicate that molecular structures may be present. There is no evidence, however, for molecular structures in $GeSe_2$ films.

I. INTRODUCTION

It is well known that the structure and properties of amorphous semiconductors are sensitive to the method of preparation.[1] For example, evaporated films of germanium and arsenic chalcogenides have x-ray-diffraction and optical absorption properties that are significantly different from the corresponding bulk glasses.[2-4] However, annealing at the glass-transition temperature reduces these differences, and the properties of the resulting annealed films are indistinguishable from those of bulk glasses.[2] The purpose of this paper and the following one (called Paper II) is to study the changes that occur on annealing in three materials: As_2S_3, As_2Se_3, and $GeSe_2$. More specifically, the local order and atomic structure are probed by extended x-ray-absorption fine structure (EXAFS) and by Raman spectroscopy. These methods together provide quantitative data on the extent of chemical ordering in these materials, and allow more precise models to be made for the thermally induced structural changes. In Paper II, the accompanying changes in optical absorption are measured and explained quantitatively on the basis of the observed structural changes.

The atomic structure of a binary alloy is determined by the atomic coordination, the relative occurrence of homopolar and heteropolar bonds, and the bonding topology. The chalcogenide glasses, quenched from the melt, form chemically ordered networks at the compositions As_2S_3, As_2Se_3, and $GeSe_2$.[5] The Ge, As, and chalcogen atoms are four-, three-, and twofold coordinated, respectively, and homopolar bonds are highly suppressed. In consequence, the local order is described by specific atomic clusters which are As-S_3 and As-Se_3 pyramidal units for the As_2S_3 and As_2Se_3 glasses and Ge-Se_4 tetrahedral units for the $GeSe_2$ glass.[6-8] In alloy compositions which are chalcogen rich from As_2S_3, As_2Se_3, or $GeSe_2$, the pyramidal and tetrahedral units are preserved, but chalcogen-chalcogen bonds are introduced into the network.[5,6] When the chalcogen fraction is sufficiently high, S_8 or Se_8 rings are known to exist.[5] In As- or Ge-rich compositions, the pyramidal and tetrahedral units are no longer completely preserved. Instead, in As_xS_{1-x} when $x>0.4$, the glass is apparently composed of only As-S_3 and S_2As-AsS_2 units. Similarly, in Ge_xSe_{1-x}, when $0.33<x<0.40$, the glass is composed of Ge-Se_4 and Se_3Ge-$GeSe_3$ units.[9] The chemical order in As-rich As_xSe_{1-x} glasses has not yet been established, and random-bonding configurations may occur.[5]

While the local atomic clusters exhibit strong effects on the vibrational spectra, the topology must also be considered. Thus the bulk glasses are believed to be formed into a fully cross-linked random network connecting the atomic units. In $GeSe_2$, Raman measurements indicate that 12-membered rings (Ge_6Se_6) form the basis of the network.[10,11] While ring structures certainly exist in the As-chalcogenide glasses, no features in the vibrational spectra have as yet been assigned to these structures.

Some indications of the structure of the evaporated films are provided by the x-ray-diffraction studies of deNeufville *et al.*[2] and Apling *et al.*[3] They show that in As_2S_3 thermal annealing causes a large reduction in strength, as well as a slight

shift in position of the first diffraction peak near 1 $Å^{-1}$, and they suggest that polymerization of a molecular species during annealing provides an explanation of this striking result. Raman studies by Solin and Papatheodorou[12] support this proposition. Furthermore, Apling *et al.*[3] find As-As bonds in as-deposited films, limiting the types of molecules that may be involved. In our work, we obtain more evidence to support this description of the structural transformation in As_2S_3, and develop a more detailed model of the process and the related processes in As_2Se_3 and $GeSe_2$.

The remainder of the paper is presented in three parts. In Sec. II the details of our experiments and the methods of analysis, particularly for the EXAFS studies, are described. Our results are presented in Sec. III. The implications of the data, for both the chemical order and the topology of evaporated and annealed films, are discussed in Sec. IV.

II. EXPERIMENTAL CONSIDERATIONS

A. Sample preparation and composition

The films were evaporated from a tantalum boat onto polyamide (Kapton) or Corning 7059 glass substrates held near room temperature, after a base pressure of 1×10^{-6} Torr had been achieved in the deposition system. The boat temperature was chosen in each case to give a deposition rate of approximately 1 $\mu m\,min^{-1}$ when a source to substrate distance of about 8 in. was used. Samples with thicknesses ranging from 10 to 50 μm were then prepared in this way by deposition of a measured amount of material. For thicknesses above about 20 μm, the material was divided between two boats, which were heated sequentially without breaking the vacuum. The chemical composition of the deposited films established by Raman and microprobe analysis is shown in Table I.

Several samples of each material were annealed in an inert atmosphere for 1–2 h, just below the appropriate glass-transition temperature. The one exception to this procedure occurred with $GeSe_2$ samples on polyamide substrates, which were only used in EXAFS experiments. In this case, the samples could not be fully annealed because of the thermal instability of polyamide at the glass-transition temperature of $GeSe_2$ (380 °C), and a considerably lower temperature of 180 °C had to be used. Further details of the annealing conditions are shown in Table I.

B. EXAFS experiment

The measurements were carried out using the EXAFS facilities at the Stanford Synchrotron Radiation Laboratory. A ⟨111⟩ channel-cut Si crystal was used in the monochromator, the stored electron-beam energy was 2.8 GeV, and copper and nickel foils were used to calibrate the photon energy and to verify the absence of second-order beams. The samples were mounted within a radiation shield on the cold finger of a liquid-nitrogen-cooled cryostat, and temperatures in the vicinity of 85 K were obtained.

The EXAFS is manifest as a series of oscillations in the cross section for K-shell absorption, and has been discussed in detail in the literature.[13] The amplitude and phase of these oscillations are determined by the position, type, and number of the atoms neighboring the excited atom. In this work, the absorption cross section was measured in a transmission geometry. For all samples the ratio of incident to transmitted x-ray intensity was recorded as a function of photon energy from 0.9 keV below to 1.6 keV above the appropriate K edge.

Using procedures that have been described in detail elsewhere,[14] the EXAFS as a function of final-state electron momentum k was extracted from the raw data and Fourier transformed to real space. The resultant complex transform $\phi_\alpha(r)$ for the K shell of atom species α can then

TABLE I. Preparation and composition parameters for As- and Ge-chalcogenide films. The errors in the composition measurement are indicated in the parentheses.

Nominal composition	Actual composition	Deposition rate (μm/min)	Thickness (μm)	Annealing temperature (°C)
As_2S_3	$As_{42}S_{58}$ [a] (±0.5)	2	30	180
As_2Se_3	$As_{43}Se_{57}$ [b] (±1.5)	1.5	45	180
$GeSe_2$	$Ge_{33.6}Se_{66.4}$ [b] (±0.5)	1.2	45	330 [c]

[a] Determined from electron microprobe, Raman, and EXAFS measurements.
[b] Determined essentially from Raman measurements.
[c] Samples on glass substrates. Those on polyamide were annealed at ~180° C.

be expressed as a sum of contributions from ea coordination shell of atoms surrounding that atom:

$$\phi_\alpha(r) = \sum_\beta \int_0^\infty \frac{dr'}{r'^2} p_{\alpha\beta}(r') \xi_{\alpha\beta}(r - r') , \quad (1)$$

where $r > 0$ and $p_{\alpha\beta}$ is the radial distribution function of atom species β about the excited atom α. Thus ϕ is a pair correlation function convolved with a peak function $\xi_{\alpha\beta}(r)$, which involves the complex t matrix of the scattering atom β, the final-state electron lifetime, and the initial phase shift due to the excited-atom potential. Because ξ also depends on the way in which the finite range of k-space data are treated, it is important to use the same treatment for all transforms that are to be compared. In each case, we use a square window that has been Gaussian broadened with $\sigma_w = 0.7$ Å^{-1}. Previous work[15] has shown that ξ is insensitive to changes in crystal structure, local bonding, thermal effects, etc. Accordingly, our analysis of the data is based on the assumption that the ϕ differ only because of differences in $p_{\alpha\beta}(r)$ from sample to sample. Thus the shift or broadening of a peak in the $p(r)$ appears as a linear shift of the peak function in ϕ or a convolution of it with a Gaussian, respectively. ϕ is then a linear combination of $\xi_{\alpha\beta}$'s, appropriately broadened and shifted.

The analysis of the EXAFS from an unknown then proceeds in the following well-established manner.[16-18] The $\xi_{\alpha\beta}$ for each pair of excited and scattering atoms is extracted from known samples, typically the elemental materials and stoichiometric bulk glasses. A model set of $p_{\alpha\beta}(r)$ is constructed for the unknown, and used with the standard $\xi_{\alpha\beta}$'s to generate a simulated ϕ_s. This ϕ_s is compared numerically with the measured ϕ, and the model $p_{\alpha\beta}$ are adjusted to achieve agreement. The best fit is determined by a minimum in

$$R^2 = (2N)^{-1} \sum^N \frac{[\mathrm{Re}(\phi - \phi_s)]^2}{(\mathrm{Re}\phi)^2 + (\mathrm{Re}\, d\phi/dr)^2} + \frac{[\mathrm{Im}(\phi - \phi_s)]^2}{(\mathrm{Im}\phi)^2 + (\mathrm{Im}\, d\phi/dr)^2} , \quad (2)$$

where the sums are over all N data points in the range (r_1, r_2), chosen to include the major part of the peak in question. This measure of the quality of fit is a standard fractional difference least squares for the real and imaginary parts individually, except for the $d\phi/dr$ terms in the denominators. These terms have been introduced to enhance the sensitivity of R to variations in the shape of the peaks in $p(r)$ at the expense of some of its extraordinary sensitivity to position. The $p_{\alpha\beta}(r)$ which result from this analysis are the desired end products.

C. Raman experiment

Polarized Raman spectra were obtained using either 6471-, 7525-, or 7993-Å krypton-ion laser excitation, at less than 20-mW incident power. The evaporated films on 7059 glass substrates were used, and for both film and bulk-glass samples, a backscatter configuration was employed. The scattered light, which was collected at an angle of ~25° from the incident laser radiation, was dispersed using a Spex 14018 double monochromator equipped with a third monochromator. The incident laser light was polarized either parallel (H) or perpendicular (V) to the scattering plane, and focused with a cylindrical lens to a vertical line on the sample surface. The scattered light was always H-analyzed. Thus polarization selection can be determined using the HH and VH scattering configurations.

The use of low-power near-infrared or red lines in the Raman measurement is particularly important in these materials, since both thermal annealing and photoinduced structural changes can be avoided.[19] Moreover, the deep penetration of the light assures the measurement of bulk properties. Even though the incident laser penetrates through the film, scattered light from the substrate is negligible because of the low scattering efficiency and fine optical focusing.

III. RESULTS

A. EXAFS results

The Fourier transforms of the EXAFS from the As K-shell absorption are shown in Fig. 1 for an evaporated As_2S_3 thin film, both as-deposited and after annealing, and for the corresponding bulk glass. The transforms reflect the As environment in these materials. The small features below 1 Å are well understood to be artifacts of the data reduction.[14,16-18] Considering the first neighbor peak at ~1.9 Å, two effects are obvious: the annealed film and bulk glass are quite similar in nearest-neighbor environment about As, while the as-deposited film has a substantial additional feature on the large-r side of the first-neighbor peak. The small-r half of the first peak in the as-deposited film can be fit using the $\xi_{\mathrm{As\text{-}S}}$ extracted from the bulk glass (the peak at 1.9 Å in the bulk glass represents S neighbors). The feature on the large-r side of the first peak can then be examined by subtracting the fitted curve (which represents S neighbors about As) from the full r-space transform of the data. The r-space transform of the as-deposited As_2S_3 film and the subtracted curve are compared to the r-space transform of bulk amor-

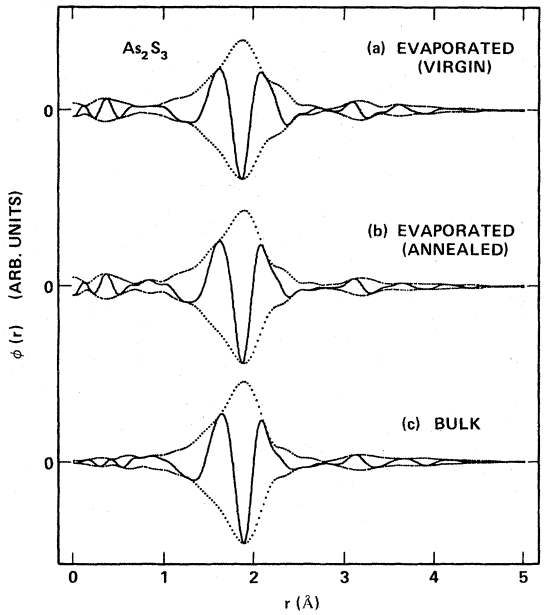

FIG. 1. Extended x-ray-absorption fine-structure results from As_2S_3 obtained from As K-shell absorption. Data are shown after Fourier transformation into real space: as-deposited film (a), evaporated film after annealing at 180 °C (b), and bulk-glass sample (c). The data are all transformed using a square window, $K = 3.7$–14.8 Å^{-1}, broadened by a Gaussian $\sigma_\omega = 0.7$ Å^{-1}. The real part (solid) and the magnitude (dotted) of the complex Fourier transform are shown. The vertical scales are arbitrary but identical.

phous As in Fig. 2.[17] The additional feature is clearly displayed in the subtracted curve. This feature is very different from that due to S scatterers [see Fig. 1c], but is precisely like that for As scatterers in pure As. This is a conclusive identification of As-As nearest neighbors in the as-deposited film. The distribution of neighbors about As for the as-deposited, annealed, and bulk-glass samples are displayed in Fig. 3. The peak widths represent the distribution in bond distances. More specifically, the first-neighbor shell about As in the as-deposited film contains 2.40 S atoms at 2.26 Å and 0.60 As atoms at 2.54 Å. Upon annealing, the first-neighbor shell changes to 2.80 S atoms at 2.27 Å and 0.20 As atoms at 2.56 Å. These remaining As atoms correspond to the reduced shoulder on the high-r side of the first peak in Fig. 1(b), and is completely accounted for by the slight departure from the nominal composition of As_2S_3 noted in Table I. The uncertainty in the number of As neighbors is ±0.05. There is also a small feature at ~3.2 Å in each sample due to As atoms at ~3.5 Å. This is an unusually well-defined peak for this distance in an amorphous solid, suggesting intermediate-range order. Our principal conclusion from this data is that the as-deposited films have a substantial number of homopolar bonds (As-As), which are largely eliminated on annealing.

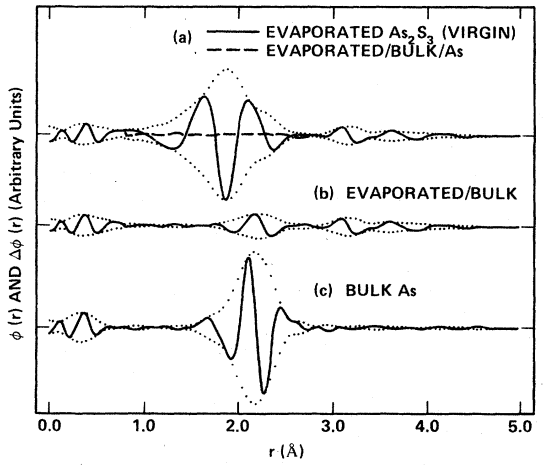

FIG. 2. Extended x-ray-absorption fine-structure data Fourier transformed into real space: as-deposited As_2S_3 film (a), as-deposited after subtracting contribution due to S nearest neighbors (b) and bulk amorphous As (c) (see Ref. 17). The real part (solid) and the magnitude (dotted) of the complex Fourier transform are shown.

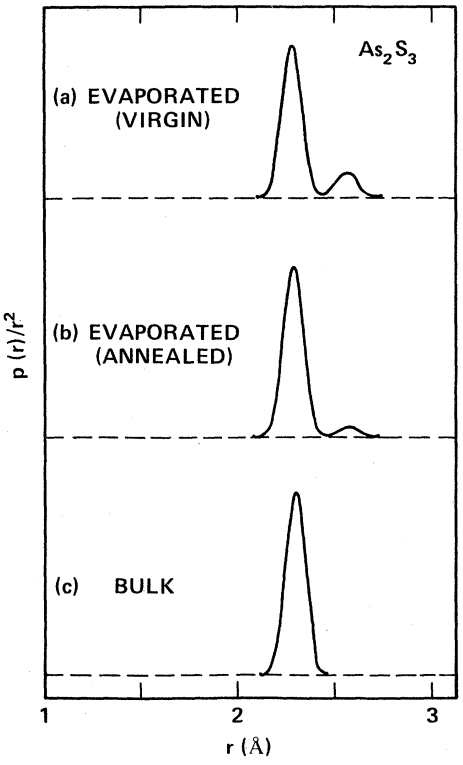

FIG. 3. Atomic density as a function of distance from the As atoms in As_2S_3. The peak at 2.55 Å is identified as As neighbors.

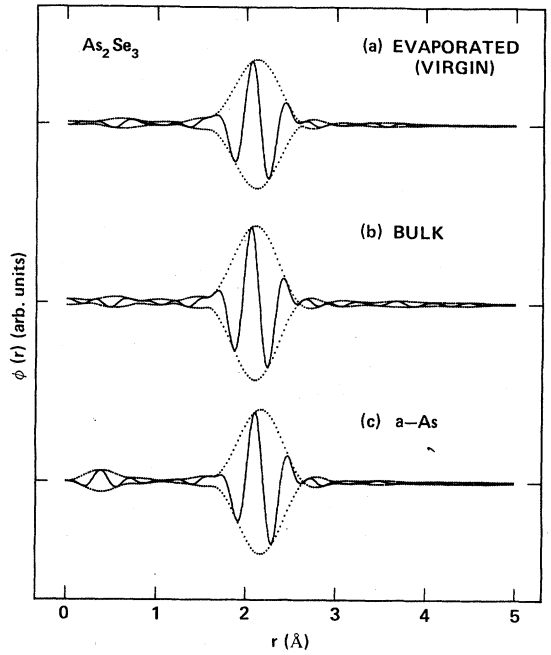

FIG. 4. Extended x-ray-absorption fine-structure real-space results of As_2Se_3 as-deposited film (a) and melt-quenched glass (b) and bulk amorphous As (c). All spectra were obtained from As K-shell absorption. The data are all transformed using a square window, $K = 3.5–12.05$ Å^{-1}, broadened by a Gaussian, $\sigma_\omega = 0.7$ Å^{-1}. The real part (solid) and the magnitude (dotted) of the complex Fourier transform are shown. The vertical scales are arbitrary but identical.

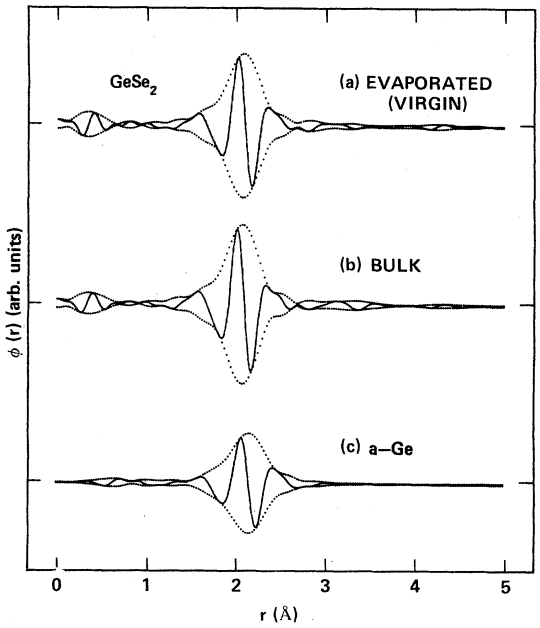

FIG. 5. Extended x-ray-absorption fine-structure real-space results of $GeSe_2$ as-deposited film (a) and melt-quenched glass (b) and amorphous Ge (c) (see Ref. 14). All spectra were obtained from Ge K-shell absorption. The data are all transformed using a square window, $K = 4.6–16.1$ Å^{-1}, broadened by a Gaussian, $\sigma_\omega = 0.7$ Å^{-1}. The real part (solid) and the magnitude (dotted) of the complex Fourier transform are shown. The vertical scales are arbitrary but identical.

The EXAFS measurements on As_2Se_3 and $GeSe_2$ cannot, however, be unambiguously interpreted. The r-space transform of the EXAFS on the As K shell for as-deposited film and bulk-glass samples of As_2Se_3 are compared to the r-space data of amorphous As in Fig. 4. The corresponding data for $GeSe_2$ are shown in Fig. 5. Because the scattering signals of the constituents are nearly identical in shape and position, an analysis like that used for As_2S_3 films is not possible. Consequently, the analysis was limited to a simple question: does adding homopolar bonds improve the comparison between the bulk glass and the as-deposited film? In the case of As_2Se_3, the comparison between the bulk glass and the as-deposited film suggests that there may be as many as 10%–15% like nearest neighbors, compared to 20% in As_2S_3. In the case of $GeSe_2$, the EXAFS gave no indication of homopolar bonds in the as-deposited film. The uncertainty associated with this analysis for As_2Se_3 and $GeSe_2$ allows error limits of ± 10% on the homopolar coordination. We note here that, as in the case of As_2S_3, the data for the bulk glass As_2Se_3 and $GeSe_2$ indicate signal at beyond 3 Å due to second-nearest neighbors. Identification of this neighbor is not possible, however, due to the weakness of the signal and similarities in scattering shapes.

B. Raman results

Information about the local order of evaporated films is obtained by comparing the Raman spectra with those of the bulk-glass alloy system, where various atomic units have already been identified. Accordingly, our spectra for the as-deposited, annealed, and bulk-glass forms of As_2S_3 are shown in Fig. 6 and off-stoichiometric glasses in Fig. 7. The spectra of the films are similar to those reported by Solin and Papatheodorou,[12] and contain several relatively sharp lines imposed on a continuum background. The sharp lines of the as-deposited film decrease in intensity or disappear upon annealing, and the spectrum then more nearly resembles that of the stoichiometric bulk glass. More specifically, the spectrum of the $As_{0.42}S_{0.58}$ glass bears a strong resemblence to the annealed evaporated film. All the sharp spectral features of the as-deposited and the annealed films, except one at ~490 cm^{-1}, are evident in the spectrum of the $As_{0.42}S_{0.58}$ bulk glass. This is a definite indication that the new features arise from struc-

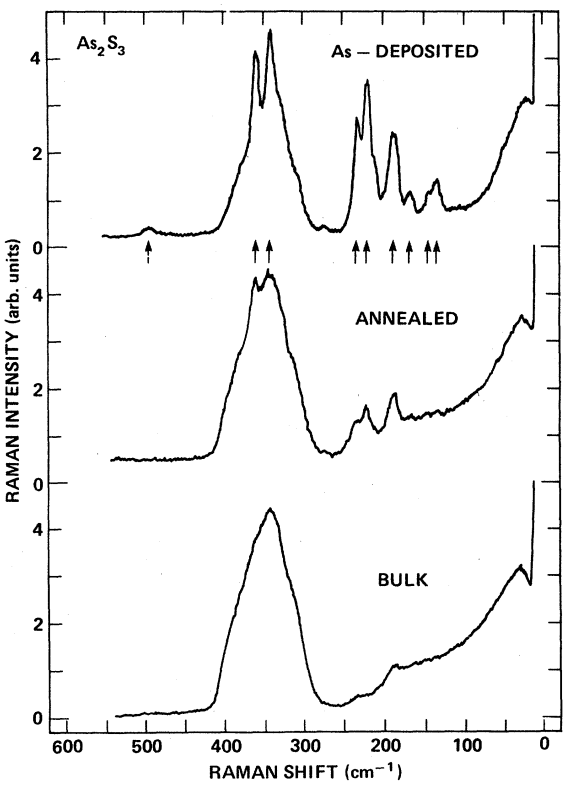

FIG. 6. *HH* Raman spectra of As_2S_3 as-deposited and annealed evaporated films and the bulk glass. The dashed arrow indicates a mode that is attributable to atomic configurations that contain S-S bonds, while the solid arrows indicate modes due to As-As bonding configurations.

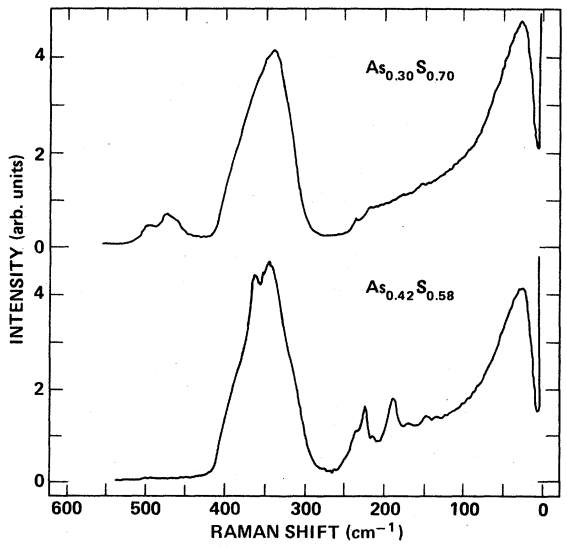

FIG. 7. *HH* Raman spectra of $As_{0.30}S_{0.70}$ and $As_{0.42}S_{0.58}$ bulk glasses. The additional features noted in Fig. 2 are evident.

tures containing As-As bonds. In fact, the observed spectral features have been shown to be consistent with modes of a local atomic structure containing two threefold-coordinated As atoms with one mutual bond and the remaining bonds terminated on S atoms (S_2As-AsS_2).[5] We note here that an As_4S_4 molecule is composed of two of these structures interconnected.[20]

The origin of the feature at 490 cm^{-1} becomes clear through a comparison with the spectrum of a S-rich bulk glass which shows a doublet in this region (see Fig. 7). The lower-frequency component has been attributed to S_8 rings, while the higher-frequency component at ~490 cm^{-1} represents S-S bonds polymerized in the glass network.[21] It is therefore evident that the evaporated film contains both As-As and S-S bonds, in agreement with EXAFS. These homopolar bonds are largely eliminated by annealing. However, the remanent As-As bond density in the annealed film shows that the sample is ~2-at.%-As rich, again in agreement with EXAFS. This result is confirmed by electron microprobe analysis. The Raman measurements also indicate that the local order around the As-As bonds is the same as in the As-rich glasses. Furthermore, a quantitative evaluation of the bond densities can be obtained from the bond statistics, as discussed in Sec. III.

The As-Se system, which bears many similarities to the As-S system, may also be expected to show new features in the as-deposited films (both systems have similar T_g, 230 °C for As_2S_3 and 180 °C for As_2Se_3). The Raman spectra of the as-deposited, annealed, and bulk-glass As_2Se_3 samples are shown in Fig. 8. While there are significant differences in the spectra of the as-deposited, annealed, and bulk samples, they are not nearly so dramatic as in As_2S_3. However, this is paralleled by the small changes in the spectra of the off-stoichiometric glasses, as demonstrated in Fig. 9. One reason for the insensitivity to composition is that the masses of As and Se are nearly identical, so that the vibrational frequencies of different atomic units can be very similar. In light of this reduced sensitivity, the weak features at ~100 and ~150 cm^{-1} and the shift of the strongest peak are indications of significant As-As bonding in the as-deposited films. These features lose intensity upon annealing, but still remain weakly evident. In addition, there is a weak shoulder at ~250 cm^{-1} that may indicate either Se-Se or As-As bonds, since both As- and Se-rich bulk-glass spectra have a shoulder here. In either case, it is clear that homopolar bonds exist in the As_2Se_3 film that are annealed to As-Se bonds. It also appears that the films are ~3-at.%-As rich, similar to the As_2S_3 evaporated films. Interpre-

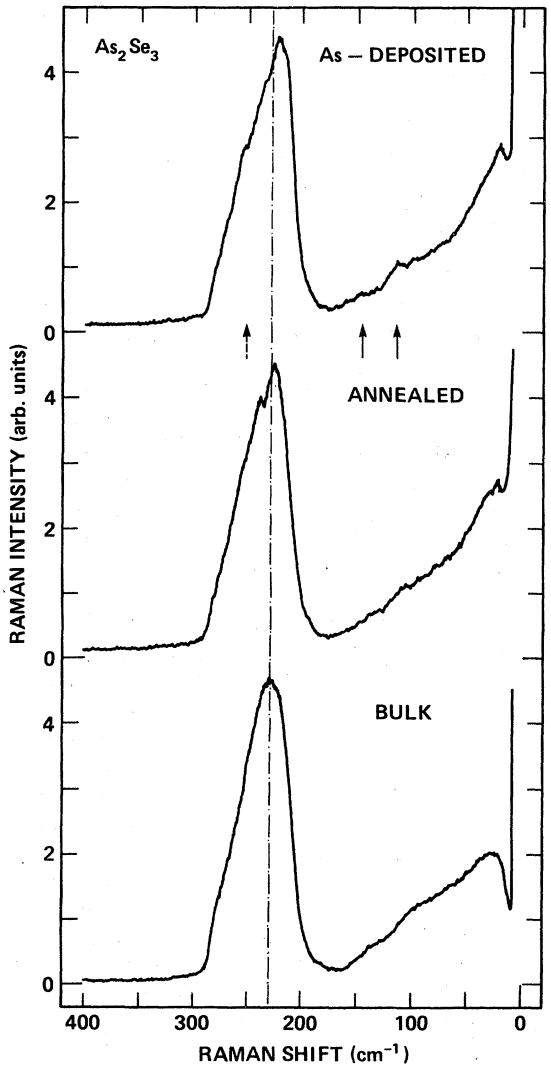

FIG. 8. *HH* Raman spectra of As_2Se_3 as-deposited and annealed evaporated films and the bulk glass. The dashed line is added to show the shift of the strongest mode. The solid arrows indicate features attributable to As-As bonding configurations, while the dashed arrow shows a shoulder that may have origin in either As-As or Se-Se bonding configurations.

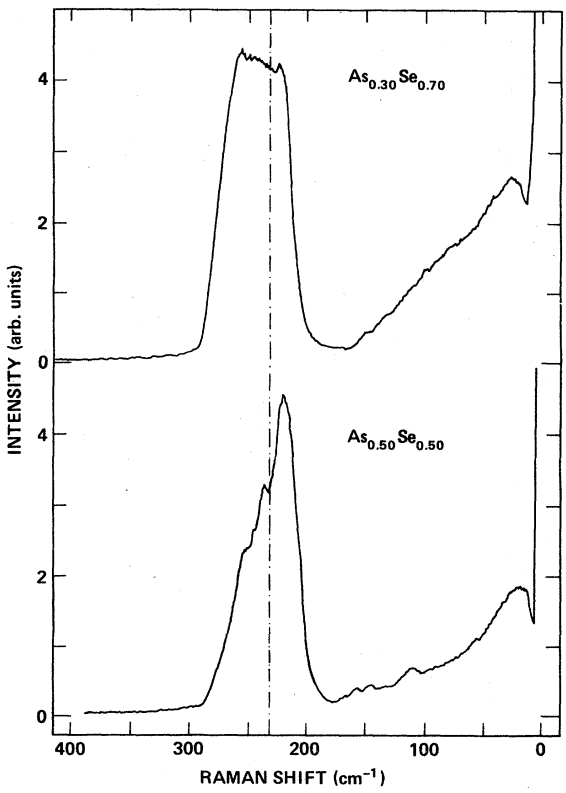

FIG. 9. *HH* Raman spectra of $As_{0.30}Se_{0.70}$ and $As_{0.50}Sc_{0.50}$ bulk glasses. The additional features noted in Fig. 4 are evident.

tation of the spectral features of the films is more difficult because the As-Se bulk-glass system has not been shown to exhibit the simple local structural units that have been used to describe the As-S system.

The spectra of the bulk glasses of Ge_xSe_{1-x} have, however, been interpreted in terms of local atomic clusters.[7,8] The Raman spectra of the as-deposited film, annealed film, and bulk-glass $GeSe_2$ are shown in Fig. 10. The mode at ~185 cm^{-1} has been identified as arising from two fourfold coordinated Ge atoms with one mutual bond and all others to Se atoms (Se_3Ge-$GeSe_3$), and the mode near 270 cm^{-1} indicates Se-Se bonds. Both spectral features are present in the as-evaporated film and clearly decrease on annealing. Thus, there is clear evidence for structures containing both Ge-Ge and Se-Se bonds. In addition, the strong mode at ~202 cm^{-1} is broadened in the film, which indicates the presence of local strain. Finally, it is evident that the stoichiometry of the annealed film is relatively close to $GeSe_2$.

A quantitive analysis of the density of each type of atomic unit observed in the Raman spectra of the films requires a knowledge of the relative scattering strengths. Fortunately, the bulk-glass systems of As-S and Ge-Se are known to be composed of only two structural units near the compounds As_2S_3 and $GeSe_2$,[5,10] and therefore, the relative concentrations of the two structures can be easily determined. In Ge-rich glasses of composition Ge_xSe_{1-x} the ratio of Se_3Ge-$GeSe_3$ units to Ge-Se_4 units, R_{Ge}, is $(2-5x)/(3x-1)$. Similarily, in As-rich glasses where the composition is As_xS_{1-x} (or As_xSe_{1-x}), the ratio of S_2As-AsS_2 to As-S_3 units, R_{As}, is found to be $(5x-2)/(4-8x)$.[22]

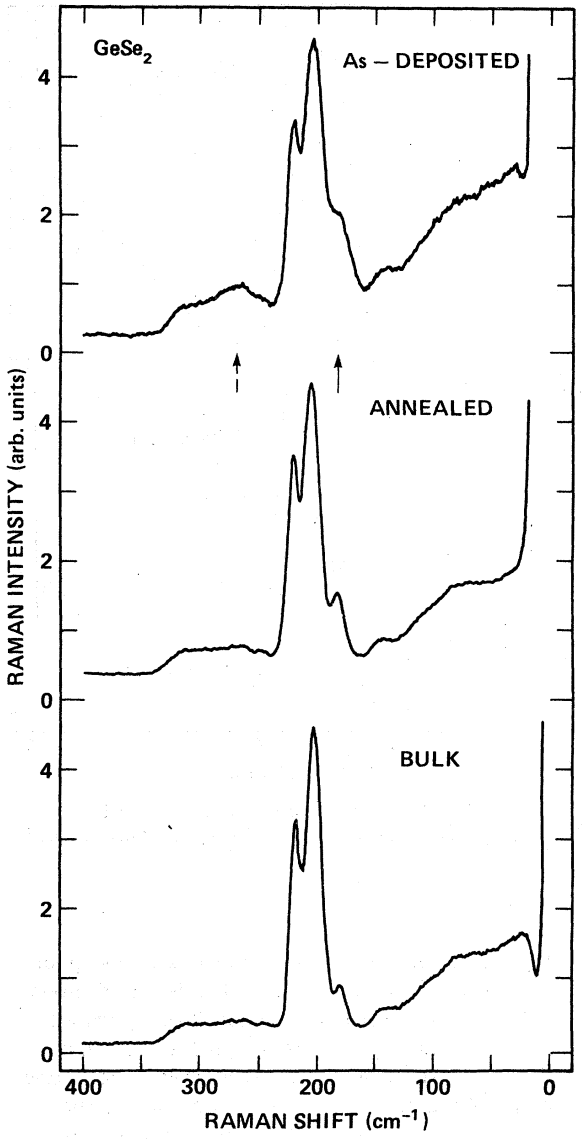

FIG. 10. *HH* Raman spectra of $GeSe_2$ as-deposited and annealed evaporated film and the bulk glass. The dashed arrow indicates a mode that is attributable to atomic configurations that contain Se-Se bonds, while the solid arrow indicates a mode due to Ge-Ge bonding configurations.

From the calculated ratio of structural units, the relative scattering strengths can then be obtained. We have considered features that arise from the structures on the As- or Ge-rich side of the stoichiometric compounds, and have calculated these ratios for the three films. The results for the films both before and after annealing are shown in Table II. Here we have assumed that the As-Se system is similar to that of the As-S system. It is interesting to note that the As_2S_3 and As_2Se_3 films exhibit significantly larger ratios than the $GeSe_2$ film; i.e., the $GeSe_2$ films show fewer homopolar bonds.

IV. DISCUSSION

A. Chemical and local order

Both the EXAFS and the Raman results demonstrate that homopolar bonds exist in the as-deposited films of As_2S_3, As_2Se_3, and $GeSe_2$. However, these measurement techniques do not provide identical information. Extended x-ray-absorption fine structure gives a direct evaluation of the average atomic coordination of each type of atom investigated, while Raman spectroscopy is sensitive to the local atomic units in the samples. The specific atomic units that contain the homopolar bonds can often be identified. Thus in this section, the EXAFS and Raman results are combined to determine the local and chemical order in the films. In Sec. IV B, the implications of these results on the topology of the network are considered.

The discussion concentrates on the coordination and local structures of the Ge and As atoms. In particular, the As-chalcogenide or Ge-Se coordination, $C_{As/Ge}$, determined from EXAFS and the ratio $R_{As/Ge}$ from the Raman, are both related to the chemical disorder of the films. The relationship of R to C is model dependent, and in the following, two different possibilities will be considered. Common to both models is the assumption that the Ge, As, and chalcogen atoms remain four-, three-, and twofold coordinated, respectively, for which there is strong experimental support.[23-25] In the first model, we assume that chemical disorder is on an atomic scale, and we define a parameter P_C which is the probability that a Ge or As atom is bonded to a chalcogen. Thus $P_c = 1$ represents the complete ordering found in bulk glasses,[5] while $P_C = 0.67$ represents completely random bonding in $GeSe_2$ (in As_2S_3 the value is 0.6). In this random-configuration model (RCM) a Ge atom may have zero to four Ge neighbors. The probability that a Ge atom has n Ge neighbors and $4-n$ Se neighbors is determined solely by P_C, and is given by

TABLE II. Values of R_{As} and R_{Ge} determined from the Raman measurements.

Nominal film composition	$R_{As/Ge}$ for as-deposited films	$R_{As/Ge}$ for annealed films
As_2S_3	0.65 ± 0.10	0.15 ± 0.02
As_2Se_3	0.91 ± 0.40	0.27 ± 0.14
$GeSe_2$	0.16 ± 0.03	0.03 ± 0.01

TABLE III. Bonding statistics, R_{As} and C_{As} for the As-chalcogenide bulk glass and films. The B and N represent the fractional bond and atomic densities. (Note that subscript C represents the chalcogenide.)

	Bulk glass As_xC_{1-x}	Film RCM	Film OCM
B_{total}	$\frac{3}{2}(N_{As}+2N_C)$	$\frac{3}{2}(N_{As}+2N_C)$	$\frac{3}{2}(N_{As}+2N_C)$
$B_{C\text{-}As}$	$2N_C$	$3N_{As}P_C$	$3N_{As}P_C$
$B_{As\text{-}As}$	$\frac{3}{2}(N_{As}-2N_C)$	$\frac{3}{2}N_{As}(1-P_C)$	$\frac{3}{2}N_{As}(1-P_C)$
$B_{C\text{-}C}$	...	$N_C-\frac{3}{2}N_{As}P_C$	$N_C-\frac{3}{2}N_{As}P_C$
Restriction	$0.40<x<0.50$	$(2N_C/3N_{As})>P_C<1$	$(2N_C/3N_{As})>P_C<1$
R_{As}	$(5x-2)/(4-8x)$	$\frac{3}{2}P_C(1-P_C)$	$(1-P_C)/(2P_C-\frac{4}{3})$
C_{As}	$2(1-x)/x$	$3P_C$	$3P_C$

$$P_C^{4-n}(1-P_C)^n 4!/n!(4-n!)\,.$$

Similarly, for the As-chalcogenide systems the probability of the equivalent As configurations are

$$P_C^{3-n}(1-P_C)^n 3!/n!(3-n!)\,.$$

It is clear that the RCM implies that the homopolar bonds occur in several different configurations. For example, in As_2S_3, not all As-As bonds occur in $S_2As\text{-}AsS_2$ units. Therefore, Raman data may reflect only a fraction of the total homopolar bond densities, and could be interpreted to give results that are very different from the EXAFS results.

The second model assumes that there are chemically ordered species in the as-deposited film. It is presumed that these reflect the structure of the vapor or the off-stoichiometric bulk glasses, a point that is discussed further in Sec. IV B. Specifically, it is assumed that the ordered species are just those observed in the Raman experiments, for example, AsS_3, $S_2As\text{-}AsS_2$, and S_2 in As_2S_3 films. In this ordered-configuration model (OCM), the probability that an As atom has one As neighbor is defined to be $3(1-P_C)$, while for the Ge-containing films the equivalent probability is $4(1-P_C)$. These definitions are convenient because the average homopolar bond density is given by identical expressions in both models. The difference between this model and the RCM is that only As-As (or Ge-Ge) coordinations of zero or unity are allowed, and by definition the Raman measurements observe the total As-As bond density.

The bond statistics for the RCM and the OCM are compared to the As- and Ge-rich bulk-glass statistics in Tables III and IV. In the formalism presented here, the relationship of the bond densities to P_C are identical for both models. While the bond densities are written in terms of both P_C and the atomic densities, these parameters must satisfy the indicated inequality relation. It is

TABLE IV. Bonding statistics, R_{Ge} and C_{Ge} for the $GeSe_2$ bulk glass and films. The B and N represent the fractional bond and atomic densities. For consistency with Table III, subscript C represents the chalcogenide which in this case is Se.

	Bulk glass Ge_xC_{1-x}	Film RCM	Film OCM
B_{total}	$2N_{Ge}+N_C$	$2N_{Ge}+N_C$	$2N_{Ge}+N_C$
$B_{C\text{-}Ge}$	$2N_C$	$4N_{Ge}P_C$	$4N_{Ge}P_C$
$B_{Ge\text{-}Ge}$	$2N_{Ge}-N_C$	$2N_{Ge}(1-P_C)$	$2N_{Ge}(1-P_C)$
$B_{C\text{-}C}$	...	$N_C-2N_{Ge}P_C$	$N_C-2N_{Ge}P_C$
Restriction	$0.33<x<0.40$	$(N_C/2N_{Ge})>P_C<1$	$(N_C/2N_{Ge})>P_C<1$
R_{Ge}	$3x-1$	$2P_C^2(1-P_C)$	$(1-P_C)/(2P_C-\frac{3}{2})$
C_{Ge}	$2(1-x)/x$	$4P_C$	$4P_C$

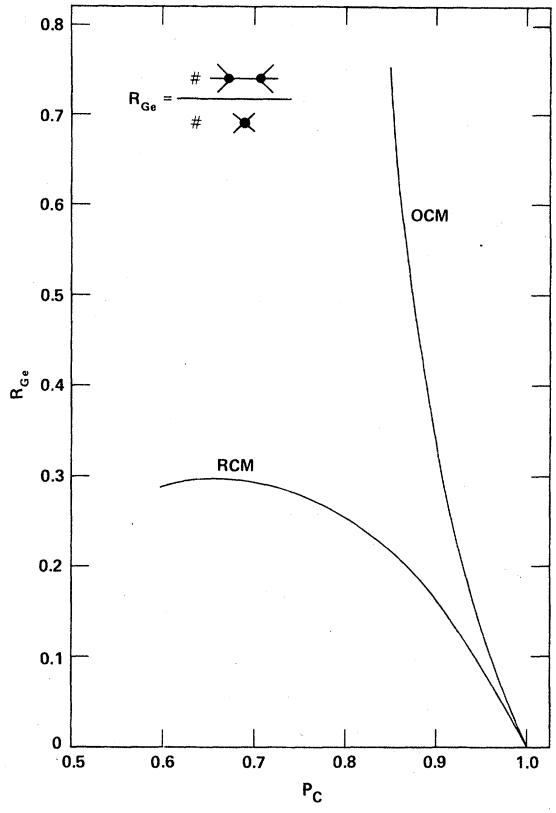

FIG. 11. Ratio R_{Ge} of Se_3Ge-$GeSe_3$ units to $GeSe_4$ units in $GeSe_2$ vs P_C for both the RCM and the OCM.

clear that the basic difference between the two models is in $R_{As/Ge}$. Since this value is used to determine the bond statistics from the Raman results, the value of P_C obtained is model dependent. The values of R_{Ge} vs P_C are shown in Fig. 11 for $GeSe_2$ for both the RCM and OCM. The Raman and EXAFS data can be used to distinguish between the two models. We proceed by first evaluating P_C from the Raman data according to both models, and the results are shown in Table V. Next, values of $C_{As/Ge}$ are found and compared with EXAFS results to determine which model provides the best fit to the data. The results for the three films are discussed separately.

The As_2S_3 evaporated films allow the most straightforward analysis because accurate data are obtained from both EXAFS and Raman measurements. From Table V, it is evident that the Raman results cannot be described by the RCM. The fact that the EXAFS results very closely agree with the Raman data if the OCM is used indicates that the As-As bonds are predominantly incorporated into S_2As-AsS_2 units. The reasons for this ordered unit are discussed in Sec. IV B including the possibility that the S_2As-AsS_2 structure is part of a molecule occurring in the vapor over As_2S_3.

The Raman measurements of $GeSe_2$ evaporated films yield several results that contrast with those of As_2S_3. There are considerably fewer homopolar bonds in the $GeSe_2$ evaporated films, and the Raman results do not exclude the possibility that the RCM applies. The EXAFS measurement of this sample also indicates a low homopolar bond density, but it is not sensitive enough to discriminate between models. However, in Paper II, it is found that $P_C = 0.92$ would account for the shift of the absorption edge on annealing. Although this result is within the error of the RCM analysis, it is possible that Ge environments with three or four Ge neighbors are not allowed, since these configurations are not found in the bulk glasses.

The results of the As_2Se_3 films are the most difficult of the three samples to analyze since neither the Raman nor the EXAFS results can be unambiguously interpreted. It is clear, however, that a significant density of homopolar bonds exists in the as-deposited films. The Raman results given in Table V seem to indicate that the film incorporates ordered structural units, although the value of R_{As} might be different if the features of the bulk glass were interpreted differently. (R_{As} was obtained based on the assumption that the

TABLE V. Values of P_C and $C_{As/Ge}$ determined from Raman scattering and EXAFS measurements. The Raman data is interpreted using a RCM and an OCM.

Film		RCM		OCM		EXAFS
		P_C	$C_{As/Ge}$	P_C	$C_{As/Ge}$	$C_{As/Ge}$
As_2S_3	As-deposited	a	a	0.81 ±0.01	2.44±0.04	2.40±0.05
	Annealed	0.88 ±0.02	2.64±0.06	0.92 ±0.01	2.76±0.03	2.80±0.05
As_2Se_3	As-deposited	a	a	0.78 ±0.04	2.35±0.15	2.65±0.3
	Annealed	0.76 ±0.15	2.29±0.4	0.88 ±0.04	2.65±0.15	$3.0^{+0.0}_{-0.3}$
$GeSe_2$	As-deposited	0.90 ±0.025	3.56±0.10	0.94 ±0.01	3.75±0.05	$4.0^{+0.0}_{-0.4}$
	Annealed	0.985±0.01	3.94±0.05	0.985±0.01	3.95±0.05	$4.0^{+0.0}_{-0.4}$

[a] No fit to the data could be obtained with the RCM.

bulk glass exhibits chemically ordered structures as in As_xS_{1-x} glasses. Another interpretation of the Raman spectra of the bulk-glass system is that the features may represent an average of several different configurations.) Again, the EXAFS results are not sufficiently accurate to distinguish between the two models. However, the similarity of the As_2S_3 and As_2Se_3 systems may also argue that the OCM at least partially applies.

B. Topology

The major thrust of this section is towards the establishment of the relation between the local order, as evidenced by the Raman and EXAFS measurements, and the overall structure of as-deposited and annealed films. Additional insight into the problem is culled from two areas: the way in which the bulk constituents evaporate and the x-ray-diffraction features of as-deposited and annealed material.

The As_2S_3 films again permit the most straightforward analysis. In Sec. IV A, we found agreement between the Raman and EXAFS results if it were assumed that the As-As bonds were all incorporated in S_2As-AsS_2 structures. The fact that these units do not occur in bulk-glass As_2S_3 strongly suggests that the chemical ordering in the films directly reflects the vapor species during evaporation. We note that S_2As-AsS_2 units occur in As_4S_4 molecules. Furthermore, the mass spectra of the vapor during As_2S_3 evaporation is dominated by As_4S_4 and S_2.[12] We therefore examine further a model in which the as-deposited film is a partially polymerized mixture of As_4S_4 and S_2 molecules.

We first note that all the Raman lines in Fig. 6 attributed to S_2As-AsS_2 structures have counterparts in the Raman spectrum of As_4S_4 liquid. The spectrum of As_4S_4 liquid taken just above the melting point of realgar is shown in Fig. 12. Moreover, the pairs of lines have identical polarization properties. This observation is not identical to the conclusion of Solin and Papatheodorou, who noted that more polarized modes were observed than could be accounted for by their group-theoretical analysis for a symmetric As_4S_4 molecule.[12] Evidently, the distortions of the molecule induced by intermolecular coupling cannot be ignored. In fact, their importance is clear from the considerable differences (~10 cm^{-1}) between the Raman spectra of the α and β forms of realgar (crystalline As_4S_4).[26]

But is this molecularlike model of as-deposited materials also consistent with x-ray-diffraction studies? Both deNeufville *et al.*[2] and Apling *et al.*[3] invoked a molecular glass model based on As_4S_6 molecules to explain the sharp first diffraction peak shown in Fig. 13, but the model was not consistent with the scattering at larger angles. Apling *et al.*[3] also suggested that the presence of some As_4S_4 and S_2 molecules could explain the shape of the first peak in the radial distribution function, but they did not compare this model

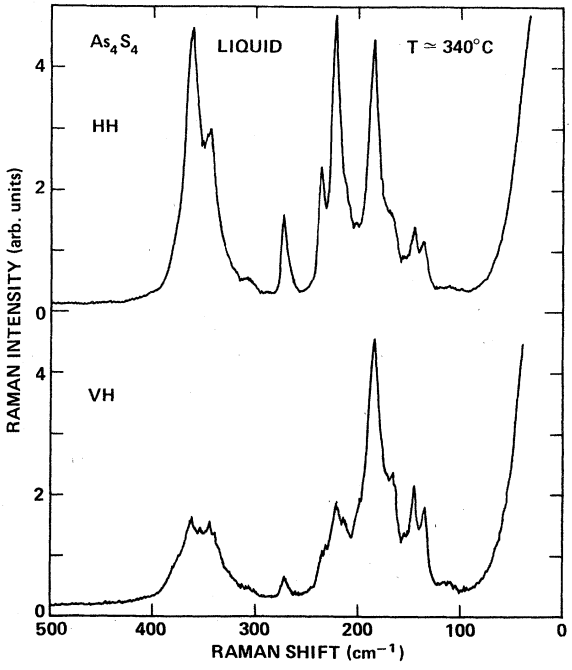

FIG. 12, *HH* and *VH* Raman spectrum of realgar (As_4S_4) liquid. The sample was contained in a sealed quartz ampoule.

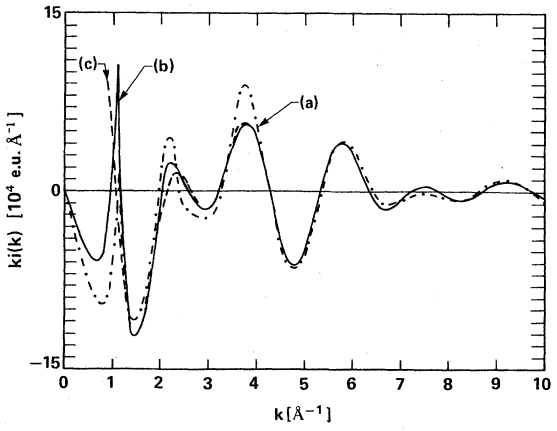

FIG. 13. Reduced scattered intensity $ki(k)$, vs k: measured on an evaporated film with composition $As_{100}S_{138}$ (Ref. 3) (a), calculated for a dense random packing of As_4S_4 molecules (b) and calculated for a single isolated As_4S_4 molecule (c).

either with the radial distribution function at larger radii or with the x-ray diffraction. Thus the limitations of their model are not well established.

For the purpose of calculation, we assume that an as-deposited film prior to polymerization consists of a random packing of randomly oriented As_4S_4 molecules (the additional sulphur atoms, of course, reside in the interstices of the structure). We obtain the appropriate packing fraction of this system by using the molecular diameter of an As_4S_4 molecule in realgar and the mass density assignable to such molecules. Then, the intensity $I(k)$ scattered by the As_4S_4 molecules at scattering amplitude k is calculated by the method of Egelstaff *et al.*[27] In our work, as in that of Apling *et al.*[3] the structure factor of a dense random packing is calculated by the method of Percus and Yevick[28] for the appropriate molecular diameter and packing faction, here 6 Å and 0.46, respectively. Similarly, the form factors, f_i for the ith atom, of Cromer and Waber were used.[29] The results, displayed as

$$k\,i(k) = k\left(I(k) - \sum_i f_i^2\right),$$

are normalized to the formula unit $As_{100}S_{100}$, and are compared in Fig. 13 with an experiment on $As_{100}S_{138}$. We have shown that correlations involving the additional sulphur atoms have no qualitative effect on our calculation, and our conclusions can safely be based on the sulphur-deficient system.

Several points should be noted. First, the locations of all of the peaks and valleys match exactly although there is some disagreement in their amplitude, particularly at low k. Second, the $k\,i(k)$'s of the packing and of an isolated As_4S_4 molecule are identical beyond about 3 $Å^{-1}$, and both closely resemble in phase and magnitude the experimentally measured $k\,i(k)$. We conclude, therefore, that the order within an As_4S_4 molecule is a good representation of the order in the as-deposited film over similar distances. Third, the peak near 2 $Å^{-1}$ is at lower k in the packing than in the isolated molecule. We would suspect, therefore, that this effect would be removed by polymerization and that the peak near 2 $Å^{-1}$ would shift to higher k as a result of annealing. This effect has been observed. Finally, the first peak near 1.1 $Å^{-1}$, which is induced solely by the packing, is far too large in our model. This effect occurs for two reasons. At low k, the long-range correlations are emphasized and our model cannot be expected to correctly incorporate them. A more important reason, however, is that both the EXAFS and Raman results indicate that the coordination of each arsenic is by 2.4 S and 0.6 As atoms on the average, whereas the completely molecular model has each As atom bonded to two S and one As atoms. Our model must therefore be allowed to polymerize in some regions, and it seems reasonable that a reduction in intensity of the first peak would result. (We note that the remaining peak near 1.3 $Å^{-1}$ in As_2S_3 glass or fully annealed film arises from correlations within a continuous network, and is not to be thought of as the remnant of the intermolecular correlations.)

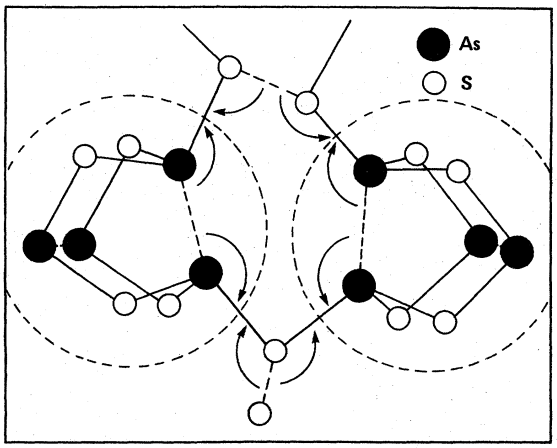

FIG. 14. Schematic representation of the mechanism by which As_4S_4 molecules and sulfur molecular units polymerize to form an As_2S_3 continuous network.

How does polymerization occur within the framework of our model? Evidently the change in local order as demonstrated by the x-ray scattering beyond 3 $Å^{-1}$ is small, yet many of the As-As and S-S bonds must disappear. From a consideration of Fig. 14, the mechanism by which these apparently opposing requirements are achieved becomes clear. Two As_4S_4 molecules are shown in close proximity to an S_2 molecule. (Of course, the sulphur pair could equally well be part of a chain or another molecular unit.) This occurs in many parts of the structure—in fact, at almost all interstices. Polymerization is then indicated by the arrows. One S atom is thus incorporated into each As_4S_4 molecule and by a repeat of this and other related processes that can easily be envisaged, a network of composition As_2S_3 can be constructed. The As-As and S-S bonds have disappeared, yet the atomic movement has been minimal!

The situation in As_2Se_3 is less well defined for a number of reasons. The features in the Raman spectra of the glass have not yet been assigned to specific structural units, and it was therefore an assumption in Sec. III B that the additional features in the spectra of the as-deposited film originated

from Se_2As-$AsSe_2$ units. Nevertheless, this approach did lead to the conclusion that the type and amount of chemical disorder are quite similar in both as-deposited As_2S_3 and As_2Se_3. The mass spectra of Leadbetter *et al.*[30] on the vapor above As_2Se_3 are also more complicated. In this case, a considerable number of As_4, As_3Se, and As_2Se_2 molecules were observed in addition to Se_2 and As_4Se_3 molecules. Although this complexity might be induced by additional fragmentation in the mass spectrometer, any model for a molecular glass is potentially more complicated. Nevertheless, a large decrease in strength and a shift to higher angles is observed for the first peak in the x-ray-diffraction curve as a result of annealing.[2] It therefore seems reasonable that a qualitatively similar explanation to that in As_2S_3 might be applicable here, but based perhaps on a distribution of molecular types.

The situation in $GeSe_2$ is quantitatively and perhaps qualitatively different. For example, there is the significant difference between the percentages of wrong bonds in $GeSe_2$ and As_2Se_3 or As_2S_3, as shown in Table V. Perhaps this is indicative of the difficulty of forming and evaporating simple molecular clusters of $GeSe_2$. Certainly a mass spectrographic study of the evaporant above $GeSe_2$ would be of some interest. It is also tempting to associate this quantitative difference with the qualitative one obtained in x-ray-diffraction studies of Ge_xS_{1-x} glasses by Cervinka and Hruby.[31] In those materials, a diffraction peak whose intensity decreases with x occurs near 1.1 $Å^{-1}$ and has an intensity in GeS_2 glass that is considerably larger than that in As_2S_3 glass. It is unlikely, however, that its origin may be explained by a molecular glass model, so that the possibility must be considered seriously that the similar peak in as-deposited $GeSe_2$ films originates from correlations within a 4:2 coordinated network. In the following, we propose a model that seems consistent with these results.

Our model is based on an observation by Nemanich *et al.*[10] that $GeSe_2$ glasses contain Ge_6Se_6 rings, within which the six Ge–Ge four-bond neighbor distances are constrained to be close to 6 Å. [The Ge–Ge four-bond distance corresponds to Ge(-Se-Ge-Se-)Ge linkages in the rings.] A typical ring is shown in Fig. 15. This situation is quite different from As_2S_3, for example, in which the rings are more distorted and high-order-bond neighbor distances have a larger spread.[23] Intuitively, this dramatic difference must arise from the fewer spatial constraints on a system with 3:2 bonding as opposed to 4:2 bonding. We therefore argue that the repetition of 6 Å correlations throughout the structure will, from the Debye formula, for example, as argued by deNeufville *et al.*[2] lead to strong scattering near 1.3 $Å^{-1}$. We can also test the consistency of this model with x-ray data by comparing the intensity scattered by a ring with experimental measurements beyond the first peak. The positions of the atoms in the ring were determined from a ball and stick model, where the Ge atoms exhibited tetrahedral coordination and the bond angle at the two-fold coordinated Se atoms was 90°. In order to obtain the correct composition dependence, an additional Se atom was attached to each Ge atom of the Ge_6Se_6 ring. The calculation proceeds exactly as before. (Of course, the first peak will not be reproduced in such a calculation because it depends on correlations between rings.) The result for the Ge_6Se_{12} ring structure is shown in Fig. 15, and compared to the experimentally measured but uncorrected scattered intensity of Fawcett *et al.*[25] The agreement between the calculated and experimental features is excellent. We have found, moreover, that this level of agreement does require atomic correlations that extend considerably beyond the basic $GeSe_4$ tetrahedron.

There are numerous predictions based on this model. First, any chemical disorder present in an evaporated film is part of a network and occurs accidently. This is in direct contrast to the situ-

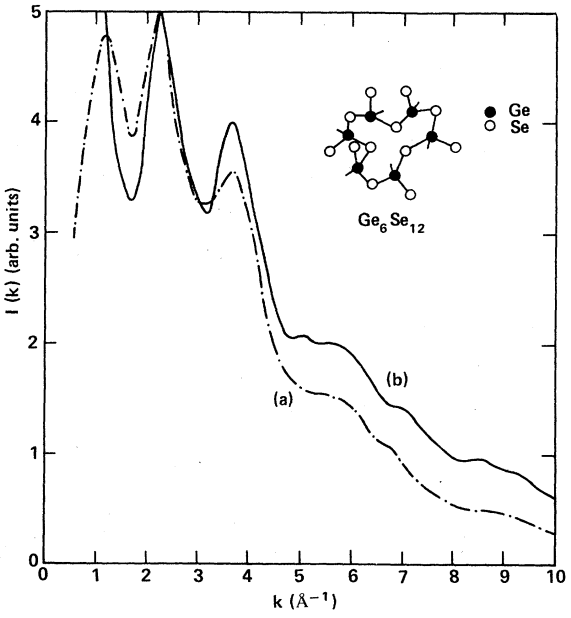

FIG. 15. Scattered intensity $I(k)$ vs k: measured on an evaporated film with composition $GeSe_2$ (Ref. 24) (a) and calculated for the Ge_6Se_{12} ring (b) shown in the insert. Note that the experimental data were not corrected for multiple scattering, etc., and the calculated experimental curves were arbitrarily normalized at the peak near 2.2 $Å^{-1}$.

ation in As_2S_3, in which the chemical disorder is a necessary part of the deposition process and chemical ordering occurs only by polymerization. Second, the peak near 1.1 $Å^{-1}$ should not be affected significantly by annealing, if the number of wrong bonds is small, and if anything should be larger in the annealed film. Again, this is a clear difference between the behavior of this and a molecular model. Third, a decrease in the intensity of the first diffraction peak is expected with increasing x in Ge_xS_{1-x} glasses, for instance, since the number of Ge(-S-Ge-S-)Ge distances will be decreased by the increase in the number of poorly defined Ge(-S-Ge-Ge-S-)Ge distances. This again is a noted feature of Cervinka and Hruby's work on Ge_xS_{1-x}.[31]

V. SUMMARY

The local order and topology of evaporated and annealed films of As_2S_3, As_2Se_3, and $GeSe_2$ have been investigated. Both Raman and EXAFS measurements show that evaporated films contain a substantial density of homopolar bonds which are mostly eliminated by annealing. Two models for the incorporation of homopolar bonds are analyzed. The first assumes that evaporation leads to a randomization of the possible bonding configurations. The second assumes that only specific atomic units occur, which are derived from the vapor species. Calculation of bonding statistics demonstrates that a combination of EXAFS and Raman measurements can distinguish between the two models. We conclude that in evaporated As_2S_3, the homopolar bonds occur only in S_2As-AsS_2 units. A similar ordered unit is possible in As_2Se_3. However, evaporated $GeSe_2$ is apparently more random.

It is argued that the presence of ordered units in the films is a consequence of the specific vapor species that occur during evaporation. In the case of As_2S_3, a model is analyzed in which As_4S_4 molecules and S-rich units are partially polymerized in the film. This model is shown to give x-ray diffraction in good agreement with experimental observations. The data suggest that evaporated $GeSe_2$ does not contain well-defined molecular species.

ACKNOWLEDGMENTS

We are grateful to G. Lucovsky for many helpful discussions, and to R. Geils and Z. Jan for preparation of the glasses. We thank the authors of Refs. 14 and 17 for the use of their EXAFS data on a-Ge and a-As, respectively. Some of the experimental results incorporated in this work were obtained at the Stanford Synchrotron Radiation Laboratory with the financial support of the NSF (under Contract No. DMR7727489), in cooperation with the Dept. of Energy.

[1]See, for example, in *Proceeding of the Fifth International Conference on Amorphous and Liquid Semiconductors*, edited by J. Stuke and W. Brenig (Taylor and Francis, London, 1974).
[2]J. P. deNeufville, S. C. Moss, and S. R. Ovshinsky, J. Non-Cryst. Solids 13, 191 (1974).
[3]A. J. Apling, A. J. Leadbetter, and A. C. Wright, J. Non-Cryst. Solids 23, 369 (1977).
[4]J. Shirafuji, G. I. Kim, and Y. Inuishi, Jpn. J. Appl. Phys. 16, 67 (1977).
[5]G. Lucovsky, F. L. Galeener, R. H. Geils, and R. C. Keezer, *The Structure of Non-Crystalline Materials*, edited by P. H. Gaskell and E. A. Davis (Taylor and Francis, London,1977), p. 127.
[6]G. Lucovsky, Phys. Rev. B 6, 1480 (1972).
[7]P. Tronc, M. Bensoussan, and A. Brenac, Phys. Rev. B 8, 5947 (1973).
[8]G. Lucovsky, R. J. Nemanich, S. A. Solin, and R. C. Keezer, Solid State Commun. 17, 1567 (1975).
[9]G. Lucovsky, R. J. Nemanich, and F. L. Galeener, *Proceedings of the Seventh International Conference on Amorphous and Liquid Semiconductors*, edited by W. E. Spear (University of Edinburgh, Edinburgh, 1977), p. 130.
[10]R. J. Nemanich, S. A. Solin, and G. Lucovsky, Solid State Commun. 21, 273 (1977).
[11]R. J. Nemanich, Phys. Rev. B 16, 1655 (1977).
[12]S. A. Solin and G. N. Papatheodorou, Phys. Rev. B 15, 2084 (1977).
[13]See, for example, F. W. Lytle, D. E. Sayers, and E. A. Stern, Phys. Rev. B 11, 4825 (1975); E. A. Stern, D. E. Sayers, and F. W. Lytle, *ibid.* 11, 4836 (1975).
[14]T. M. Hayes, P. N. Sen, and S. H. Hunter, J. Phys. C 9, 4357 (1976).
[15]Although this point has been discussed by P. A. Lee and G. Beni [Phys. Rev. B 15, 2862 (1977)], and in several works by one of the present authors (T. M. H.), the most complete treatment to date is in a pair of papers by B. K. Teo, P. A. Lee, A. L. Simons, P. Eisenberger, and B. M. Kincaid, J. Am. Chem. Soc. 99, 3854 (1977); 99, 3856 (1977).
[16]J. B. Boyce, T. M. Hayes, W. Stutius, and J. C. Mikkelsen, Jr., Phys. Rev. Lett. 38, 1362 (1977).
[17]J. C. Knights, T. M. Hayes, and J. C. Mikkelsen, Jr., Phys. Rev. Lett. 39, 712 (1977).
[18]T. M. Hayes, J. W. Allen, J. Tauc, B. C. Giessen, and J. J. Hauser, Phys. Rev. Lett. 40, 1282 (1978).
[19]J. P. deNeufville in *Optical Properties of Solids—New Developments*, edited by B. O. Seraphin (North-Holland, Amsterdam, 1976), p. 437.
[20]R. W. G. Wyckoff, *Crystal Structures* (Wiley, New York, 1963), Vol. 1, p. 174.
[21]A. T. Ward, J. Phys. Chem. 72, 4133 (1968).
[22]R. M. White, J. Non-Cryst. Solids 16, 387 (1974).
[23]A. L. Renninger and B. L. Averbach, Phys. Rev. B 8, 1507 (1973).

[24]O. Vemura, Y. Sagara, and T. Satow, Phys. Status Solidi 32 A, K91 (1975).
[25]R. W. Fawcett, C. N. J. Wagner, and G. S. Cargill, III, J. Non-Cryst. Solids 8–10, 369 (1972).
[26]R. Zallen (unpublished).
[27]P. A. Egelstaff, D. I. Page, and J. G. Powles, Mol. Phys. 20, 881 (1971).
[28]For a discussion of the method used here, see A. C. Wright, Discuss. Faraday Soc. 50, 111 (1970).
[29]D. T. Cromer and J. T. Waber, Acta Crystallog. 18, 104 (1965).
[30]A. J. Leadbetter, A. J. Apling, and M. F. Daniel, J. Non-Cryst. Solids 21, 47 (1976).
[31]L. Cervinka and A. Hruby, in Ref. 1., p. 431.